Available online at www.sciencedirect.com

ScienceDirect

Procedia Manufacturing 11 (2017) 536 – 544

Procedia MANUFACTURING

27th International Conference on Flexible Automation and Intelligent Manufacturing, FAIM2017, 27-30 June 2017, Modena, Italy

Filament Temperature Dynamics in Fused Deposition Modelling and Outlook for Control

D. Pollard[a,]*, C. Ward[a], G. Herrmann[a], J. Etches[a]

University of Bristol – Queen's Building, University Walk, Bristol BS8 1TR

Abstract

Fused Deposition Modelling (FDM), a form of Additive Manufacture, can produce 3D components directly from CAD data. This paper investigated fluctuations in filament temperature during step changes in feed rate and start/stop motions, monitoring temperature using a thermal camera and thermistors embedded in both the block and nozzle. Temperature overshoots 12°C and 18.5°C were observed during a step increase in feed rate and a priming motion respectively. Evaluating these changes with a sintering model predicted a 20% increase in bond formation, although no significant differences of bond sizes were observed using optical measurement.

Peer-review under responsibility of the scientific committee of the 27th International Conference on Flexible Automation and Intelligent Manufacturing

Keywords: Fused Deposition Modelling; Additive Manufacture; Quality Control; Extrusion; Process Monitoring

1. Introduction

Additive Manufacturing (AM) is defined as a process of joining materials to make an object from three-dimensional model data [1]. This technique is divided into several categories, separated by input materials and the forming process used. AM has numerous advantages over conventional manufacturing; the ability to manufacture

* Corresponding author. Tel: +44 (0) 117 331 5921 (Dr. Guido Herrmann)
E-mail address: d.pollard@bristol.ac.uk

Peer-review under responsibility of the scientific committee of the 27th International Conference on Flexible Automation and Intelligent Manufacturing
doi:10.1016/j.promfg.2017.07.147

parts directly from CAD data, the capability to produce complex geometries, and reduced waste when compared to conventional subtractive manufacturing methods [2, 3].

Fused Deposition Modelling (FDM), a form of AM, involves the extrusion of molten plastic through a movable nozzle [1, 4]; a process originally developed by Stratasys Inc in 1992 [5]. In 2005, the RepRap project released open source design files for FDM systems, demonstrating its potential for low-cost desktop prototyping and manufacturing [6]. The use within industry of FDM systems has grown over the past decade due to the increasing quality and reliability of the available equipment [4].

Sandwich panels, comprised of a core placed between two face sheets of high modulus material, are common composite components in modern aircraft, providing a large proportion of secondary structures in the wing. Complex panels include features such as bolt holes, complex curvatures, and variable strength requirements [7]. Recent work has focused on exploiting the wide design space and flexibility of FDM for the manufacture of complex core geometries for sandwich panel manufacture [8, 9]. The structural properties of thin-walled FDM cores for lightweight applications has been explored in [10, 11].

Within the aerospace industry, high levels of quality assurance and control are drivers for the adoption of new manufacturing technologies; analogous with medical engineering. The Food and Drug Administration (FDA) has released draft guidance on the use of 3D printing for medical devices [12]. To certify manufacturing processes, sources of error must be identified, permitting the application of AM processes for customized, reliable, and qualified components.

Thermal modelling of the FDM process was initially conducted by Yardicimi et al. [13], modelling melt flow within a liquefier. The internal pressures of the liquefier were investigated by Bellini et al. [14], and the results were expanded on by Ramanath et al. [15] to model the internal flow for bio-polymer printing. It was found that the melt front occurs far from the nozzle, resulting in a longer time at elevated temperatures for the filament. The filament temperature and bonding has been investigated by Belleumeur et al. [17, 18], where a model and experiments evaluated the effects of processing conditions on sintered bond formation while under steady state extrusion conditions.

This paper presents the effect of the unsteady flow conditions of start, stop, and feed rate changes on filament temperature for acrylonitrile butadiene styrene (ABS) and polylactic acid (PLA). Temperatures were recorded through a thermal camera, and thermistors embedded within both the block and nozzle during step changes in feed rate and dynamic start/stop motions. An estimate of the change in sintered bond formation was then modelled, and thin-walled FDM specimen profiles optically measured to estimate bond formation. Finally, the frequency response of the block and nozzle are presented, and the challenges of temperature control for improved quality discussed.

2. Filament temperature modelling

To measure the temperature throughout the extruder, a commercially available 0.6 mm hotend [19] had an additional thermistor embedded into a hole machined into the side of the nozzle. The 2.85 mm filament was driven by a direct drive Bulldog extruder, controlled through a dSpace 1103 rapid prototyping board [20] with custom software. The step signal to drive the extruder stepper motor was produced using the inbuilt variable frequency square wave generator, and the heater cartridge controlled through the inbuilt PWM generator. The temperature recorded from the thermistors was sampled at 1 kHz, allowing the fast responses to be monitored. To investigate the response for different input signals, both the block and nozzle thermistor readings could be used as the input signal for the PI temperature controller, as it was hypothesized the nozzle would have an improved response time due to its lower thermal mass.

The filament temperature upon the extrusion, and the nozzle and block temperature was monitored using a FLIR T650 thermal camera at frame rate of 30 Hz, and analyzed with the accompanying ResearchIR software [21]. A good correlation was found between the temperatures measured by the thermistor and camera. Figure 1 shows the nozzle with the thermistor attached, and a sample image obtained from the thermal camera highlighting the observation regions around the block, nozzle, and filament during extrusion.

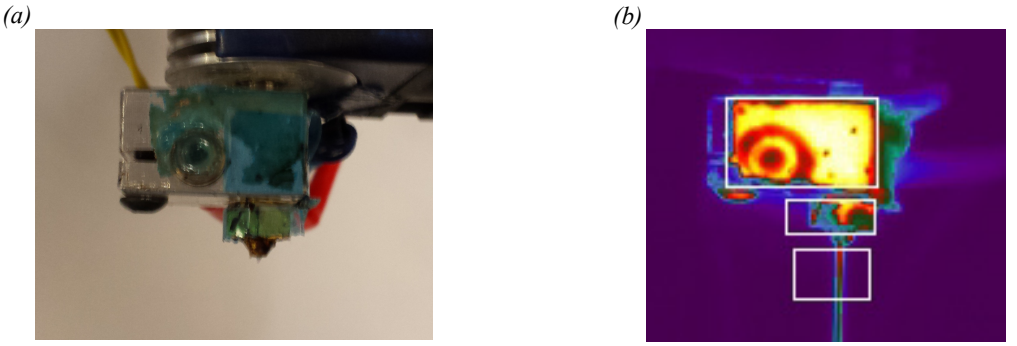

Fig. 1. *(a)* shows the thermistors inserted into the block, and the flash tape used to enable IR temperature measurements through an increase in surface emissivity. *(b)* displays an image as captured by the thermal camera.

2.1. Filament temperature during step changes in feed rate

The first test recorded the filament temperature during a step change in filament feed rate. The low and high feed rates investigated were 0.5 and 2 mm s^{-1}, corresponding to flow rates of 3.19 and 12.76 mm^3 s^{-1}. Table 1 shows the maximum temperature change and rise time of the filament due to the step change in feed rate, as measured by the thermal camera.

Table 1. Thermal response of filament due to a step change in feed rate. The Block/Nozzle Control denotes the location of the thermistor providing input to the PI temperature controller.

		ABS		PLA	
Step	Property	Block Control	Nozzle Control	Block Control	Nozzle Control
Low – High	Temperature change (°C)	9.85	5.51	3.19	2.55
	Rise time (s)	0.33	0.24	0.50	0.31
High – Low	Temperature change (°C)	-11.15	-12.29	-2.52	-2.84
	Rise time (s)	0.60	0.55	0.56	0.38

As seen in Table 1, the high-low step caused an increase in filament temperature, and the low-high step a decrease. The opposite effect was observed for the nozzle and block temperatures; a low-high step decreased the recorded temperatures due to the increased heating requirements to compensate for the increased mass flow. The step change in feed rate forced the melt front closer to the nozzle, expelling the plastic within the melt zone; showing a movement of melt front towards the nozzle. This indicated the melt zone within the extruder was maintained at a higher temperature than the filament upon the point of measurement.

The use of the nozzle control was shown to shorten the rise time of the filament temperature, and decrease the total step size for the low-high step. The ABS filament was found to have a larger step size than the PLA, and a shorter rise time. A difference in absolute settled temperature differences after the step change in feed rate was also observed; the ABS had an average settled temperature difference of 1.2°C for block control and 7.5°C for the nozzle control, compared to 8.5°C and 9.2°C for the PLA block and nozzle control respectively. In the analysis of the input PWM signal to the heater block, the nozzle temperature responded significantly faster than the block temperature following a change in feed rate, causing a faster change in the heater PWM signal. A secondary observation was there was a higher chance of fluctuations around the set point temperature for nozzle control. This was due to the increased distance between the heater location in the block and the nozzle thermistor, causing an increased delay when compared to the block mounted thermistor, a cause of control instability.

2.2. Filament temperature during retraction and priming motions

Start/stop tests were conducted through factorial investigations modifying parameters related to the retraction and priming motions, and a pause length of 1 or 10 s between the stop and the restart; the pause reflecting the effect of different travel times between the deposition of adjacent roads, or a fast surface scan of the previously deposited layer. Retraction and priming are commonly used within FDM systems; retraction to stop extrusion, avoiding unwanted deposition during travel through movement of the melt front away from the nozzle orifice, and priming to return the melt front to initiate extrusion when required. The feed rate profile of the dynamic motions of retraction and priming are shown in Figure 2, where a negative feed rate is used to retract the filament, and positive feed rate to prime for the next extrusion. Two factorial investigations were conducted, with the factors for both investigations shown in Table 2. The first experiment, with PLA, investigated the effect of different durations of retraction/priming, and the length of the pause between retraction and priming motions. The low values for the speed multiplier and feed rate were used. The second experiment, with ABS, investigated the effect of feed rate and the speed multiplier; the change in duration of the retraction/priming motions whilst maintaining the same filament travel distance. The high level involved increasing the retraction/priming speed, whilst reducing the duration of the motion. Each factor combination was tested three times, in a randomized order. The PI temperature controller used an input signal from the block-mounted thermistor.

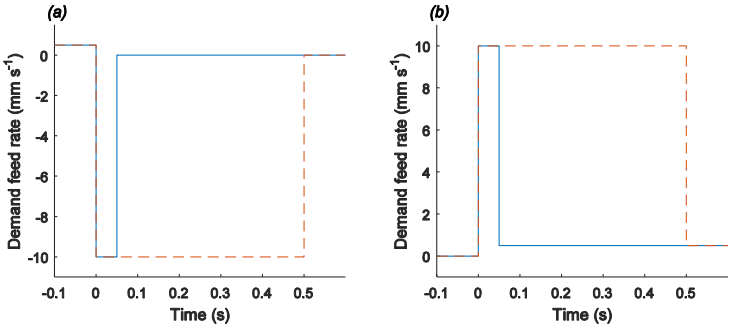

Fig. 2. Feed rate during high (dashed line) and low (solid line) retraction/priming motions. A positive feed rate denotes the filament was driven towards the nozzle orifice for extrusion. (a) shows the retraction profiles, used to stop extrusion, (b) shows the priming profiles, used to restart extrusion.

Table 2. High and low factors investigated during testing of retraction/priming motions.

Factor	Low value	High value
Retract duration	0.05 s	0.5 s
Prime duration	0.05 s	0.5 s
Pause time	1 s	10 s
Speed multiplier	x1	x4
Feed rate	0.5 mm s^{-1}	2 mm s^{-1}

It was found that the pause had no significant effect on the filament temperature response after the priming action; all presented results have the high pause time depicted for clarity. Figure 3(a, b) shows the temperature response for low and high retraction durations, with a high pause and low prime values. No significant delay was observed in the temperature reaching the steady value, as seen in Figure 3(a), while a high retract coupled with a low prime, Figure 3(b), has a long delay, as expected due to the movement of the melt front.

Figure 3(c, d) depicts filament temperature responses for low and high retraction durations, with high pause and high duration priming. There was no significant delay for either setting reaching the previous extrusion temperature, however there was a significant overshoot in Figure 3(c), where low retraction and high prime values were used.

This was a similar effect to that observed in Section 2.1, where a low-high step caused an increase in filament temperature. Values for overshoot and settling times of these tests are presented in Table 3.

A comparison between Figure 3(a) and (d) shows the effects of modifying both retraction and priming durations. Both settings provided a fast temperature response with low overshoot; implying for a constant temperature deposition, the priming and retraction motions should have equal filament travel for deposition at constant temperatures.

The results of the second investigation, with ABS plastic, are shown in Figure 4, and the overshoot and settling times in Table 3. Through comparison of Figure 4(a) and (b), no significant difference in temperature response time was observed when the speed multiplier was applied. The higher speed multiplier setting reduced temperature fluctuations after the priming action occurred (between 20 and 25 s), but significantly increased the overshoot.

Figure 4(d) depicts the effect of an increased flow rate, with identical retraction, pause, and priming parameters to those used as Figure 4(b). An increased overshoot was observed for the higher flow rate, with a longer settling time.

Table 3. Overshoot and settling times for selected figures

	Figure 3(c)	Figure 3(d)	Figure 4(a)	Figure 4(b)	Figure 4(c)	Figure 4(d)
Overshoot (°C)	10.1	2.4	12.9	8.1	15.1	18.5
Settling time (s)	0.81	0.60	0.52	0.66	0.99	6.77

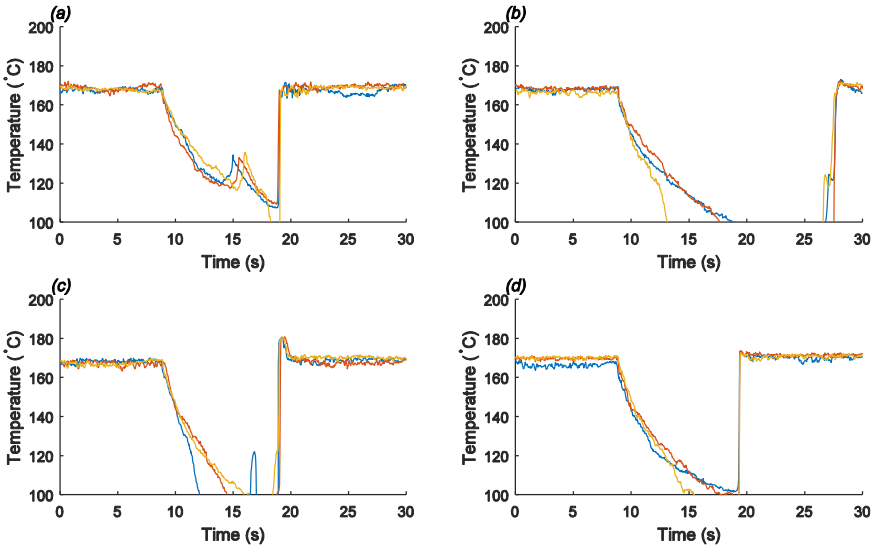

Fig. 3. Filament temperature response during retraction and priming tests for PLA. All plotted responses have a high pause time of 20 s. (a) shows responses for a low retract and low prime, (b) shows high retract and low prime. (c) shows low retract and high prime, (d) shows high retract and high prime

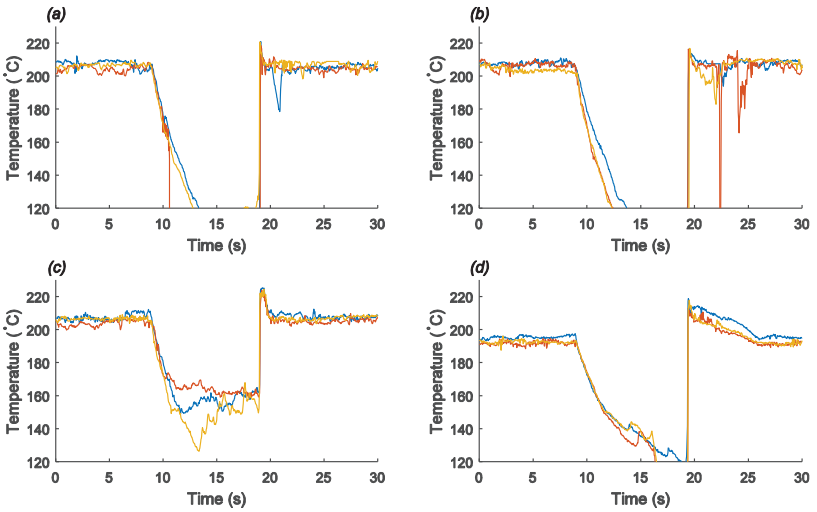

Fig. 4. Filament temperature response during retraction and priming tests for ABS. (a) shows high retraction and high prime, with a high level speed multiplier; the movement time was decreased and speed increased by a factor of 4. (b) shows high prime and retraction with no speed multiplier; analogous to Figure 3(d). (c) shows the combined effect of low retraction and high prime, analogous to Figure 3(c), (d) shows the effects of an increased feed rate of 2 mm s-1. Overshoot and settling times are shown in Table 3.

3. Measurement of bonding levels within thin walls

To estimate the effect of the recorded temperature fluctuations, as in Section 2, a numerical sintering model was applied to predict the filament bonding. Thin walls were then manufactured using FDM with the temperature during the build monitored with a thermal camera, and the surface scanned with an optical coordinate measuring machine to identify if changes in bond formation were visible.

3.1. Effect on sintering bonding

The bond formation caused by the polymer sintering effect was evaluated with a commonly used model presented by Bellehumeur et al. [17, 18]. Bond formation was represented by the dimensionless unit *y/*a, the ratio of half the width of sintered bond *(y)* to the filament radius *(a)* as shown in Figure 5. The cooling model, and material parameters of surface tension and viscosity functions were derived within [17] for ABS P400. While this was a different blend of ABS to that examined here, the rheological properties provided an estimate for bond formation over a range of temperatures. It was found the material parameters and initial temperature were the parameters which had the most significant effect on the anticipated bond formation.

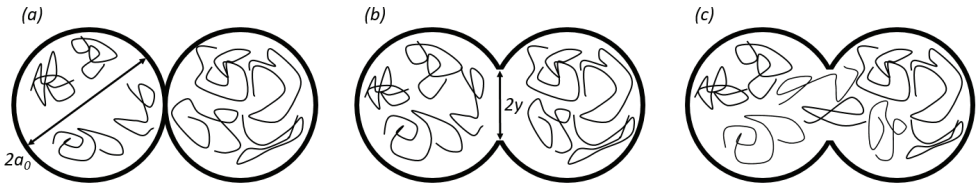

Fig. 5: The formation of a sintered bond through the movement of the polymer chains, as presented in [19]. *(a)* shows the filament instantaneously after deposition, *(b)* shows the neck growth, and *(c)* shows the sintering effect due to the movement of polymer chains.

Through variation of the initial temperatures based on the experimental results from step and dynamic tests, the expected level of sintered bond formation was calculated. Table 4 shows the results of the variations in the range found in Sections 2.1 and 2.2, with the steady state temperature evaluated at both 200 and 225°C. Table 4 shows the resulting dimensionless bond size *(y/a)* within the range of observed temperature fluctuations, and the relative change based on the steady state temperature. There was a clear change in the estimated sintered bond formation within the temperature ranges shown to occur through dynamic filament movements. This model has underestimated the bond formation, as the assumed shape of the two filaments to be sintered was cylindrical, whereas the true extruded filament formed an oval-shaped deposited road; leading to an increased initial contact area than predicted.

Table 4. Variation of dimensionless sintered bond formation based on [17] at an extruded temperature of 225°C. The italic percentages show the effect of the variation on sintered bond formation based on the steady state deposition temperature expected after the feed rate changes.

Extruded filament temperature (°C)	Variations (°C)				
	+20	+10	+0	-10	-20
y/a	0.1736	0.1612	0.1430	0.1235	0.1050
Percentage change	*21.40%*	*12.73%*	*0.00%*	*-13.64%*	*-26.57%*

3.2. Bond radii measurement

To measure the contact area between filaments, FDM was used to produce walls 50 layers high (25 mm), the thickness of a single extruded road, with the wall temperature monitored with a FLIR T650 thermal camera. Specimens were printed at a temperature of 225°C in both directions, left to right and right to left, and at two speed levels; a low nozzle speed of 8.33 mm s^{-1} with a feed rate of 0.5 mm s^{-1}, and at a high nozzle speed of 16.67 mm s^{-1} with a feed rate of 1 mm s^{-1}. Additional specimens were produced with a step change in nozzle speed from low to high values at the center point of the wall, representing the step change investigated in Section 2.1. A pause was inserted between the layers on specimens printed with higher speeds to ensure consistent layer print times of 14.5 s.

The surface profiles of the left and right sides of the specimens were measured using an Alicona InfiniteFocus 3D micro coordinate measurement machine, calibrated for a vertical resolution of 2.5 µm and a lateral resolution of 7.5 µm. Bond depth was measured from the resulting 3D model data with the Alicona IF MeasureSuite profile measurement tool, calculating the average height between the widest and narrowest points of the top ten layers of deposited filament; the lowest point measured was on the inter-layer bond line. Temperature was measured through averaging the temperature over a central 10 mm section on the left and right sides to identify if the temperature fluctuations of the start or step affected the bond formation in the central sections of the wall.

There was no statistically significant difference in wall thickness (0.91 mm) or measured bond height (174 µm) between the initial low speed sections of the step, and the specimens printed at a low and constant speed. Significant differences were observed between the measured parameters of the post-step, high speed, specimens and the constant high speed specimens; an increase of 0.02 mm in thickness and 4 µm in bond height. However, as a proportion of thickness, the observed variation in bond height was not considered to be significant. Data thus far has shown no observable differences in the temperature distribution caused by variation in filament temperature due to step changes in flow rate; a finding supported by the consistency of bond depths from optical measurement.

4. Outlook on control

Section 2.1 has shown the measured nozzle temperature had a significantly faster response to the fluctuations caused by flow rate changes than the block, implying a nozzle mounted thermistor would provide improved control over the extruded temperature. However, as observed in Section 2.1, an increased delay was evident. To quantify the response and formulate models of the temperature responses, the block and nozzle thermistor responses were recorded when a step change to the input PWM was applied to the heating element. Models were then optimized to fit the responses, and evaluated using combinations of step signals. The most suitable form of the equations through similarity to the measured response to an input signal comprising of multiple step signals, as shown in Figure 6. The

most suitable models are shown in equations *(1)* and *(2)* for the block and nozzle respectively, with the optimized coefficient values removed for clarity.

From the model responses, it was observed both nozzle and block models had a similar magnitude response, but there was a significant drop of in phase response of the nozzle model at frequencies greater than 10^{-1} rad s^{-1}. This was reflected in the increased delay between temperature input and response as observed in Section 2.1.

$$G(s) = F\frac{e^{-As} + B}{Cs^2 + Ds + E} \quad (1)$$

$$G(s) = E\frac{e^{-As} + B}{Cs + D} \quad (2)$$

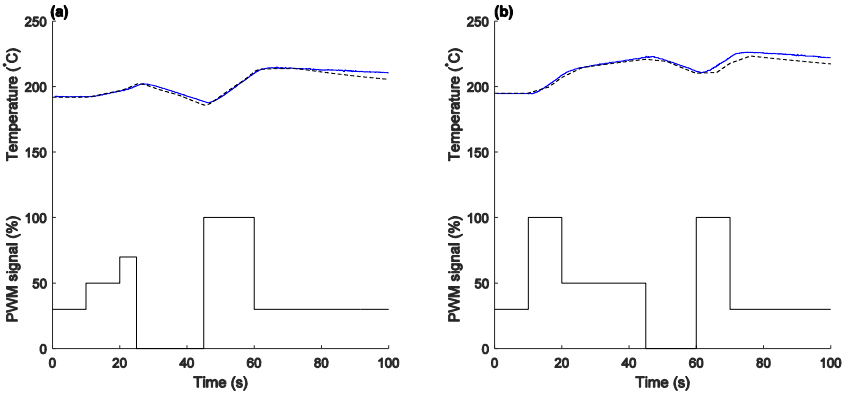

Fig. 6. Response of fitted models for the block *(a)* and the nozzle *(b*). The recorded thermistor temperature the solid line, and the model temperature estimate is shown by the dashed line. The PWM input to the heater is shown as a percentage of maximum power, two examples of the signal used to evaluate the models are depicted.

5. Conclusions

This paper has presented measurements of filament temperature fluctuations due to feed rate changes; both step changes, and priming and retraction motions used at the beginning and end of road deposition. It was found the ABS filament had higher temperature variations during all feed rate variations than PLA. In addition, a reduction in rise time was achieved through use of the nozzle-mounted thermistor for the temperature control input, as an alternative to the traditional block-mounted thermistor. However, the lag due to the increased distance between the heater cartridge and the nozzle thermistor must be compensated for to reduce steady state errors.

There was no noticeable delay in temperature rise when identical priming and retraction settings were used. An increased feed rate before the retraction and priming motions amplified the overshoot from 12.9 to 18.5°C. With a lower retraction than prime, the observed overshoot was similar to that of the low-high step test.

The application of the sintered bonding model has provided an estimate of inter-layer bonding at different filament temperatures. The model predicts significant effects on sintered bond formation within the experimental temperature ranges, an effect with implications on bonding consistency. Results from optical measurement of the surface to identify variations in bond thickness due to speed changes were inconclusive. While the sintered bonding model significantly underestimated the bond size observed in optical measurement, the true shape of extruded filament was not accounted for, and the optical methods could not identify the level of entanglement of polymer chains within the bond, which would be expected at the center of the bond.

Section 2.1 found the nozzle had a significantly larger and faster response to fluctuations in filament temperature than the block. This implies control through the nozzle would be more suitable for use for high quality components with minimum fluctuations in material temperature. However, as shown in Section 4, a significant phase delay is

present. This implies a PI controller was not suitable for such control, and more advanced algorithms would be better suited for maintaining more consistent temperatures.

In conclusion, this paper has shown there can be significant variations in filament temperature on extrusion during step changes in feed rate and priming. A sudden decrease in feed rate could cause structural weaknesses due to the lower extruded temperature. Understanding this effect is vital to part certification for aerospace industry, where a knowledge of the complete process is required. A second application would be within the medical industry, where bio-polymers require precise control over processing conditions.

Acknowledgements

This work was supported by the EPSRC Centre for Doctoral Training in Future Autonomous Robotic Systems (FARSCOPE) at the Bristol Robotics Laboratory (grant EP/L015293/1).

The data necessary to support the conclusions are included within this paper.

References

[1] ASTM Standard, ISO/ASTM 52900:2015 Additive manufacturing - General principles - terminology, ASTM F2792-10e1, 2012.

[2] Gao, W.; Zhang, Y.; Ramanujan, D.; Ramani, K.; Chen, Y.; Williams, C. B.; Wang, C. C.; Shin, Y. C.; Zhang, S. & Zavattieri, P. D. "The status, challenges, and future of additive manufacturing in engineering," *Computer-Aided Design,* vol. 69, pp. 65-89, 2015.

[3] S. Mellor, L. Hao and D. Zhang, "Additive manufacturing: A framework for implementation," *International Journal of Production Economics,* vol. 149, pp. 194-201, 2014.

[4] T. Wohlers, "Wohler's report 2013," *status: published,* 2013.

[5] S. Crump, *Apparatus and method for creating three-dimensional objects,* US Patent 5,121,329, 1992.

[6] R. Jones, P. Haufe, E. Sells, P. Iravani, V. Olliver, C. Palmer and A. Bowyer, "RepRap--the replicating rapid prototyper," *Robotica,* vol. 29, no. 01, pp. 177-191, 2011.

[7] C. Ward, K. Hazra and K. Potter, "Development of the manufacture of complex composite panels," *International Journal of Materials and Product Technology,* vol. 42, no. 3-4, pp. 131-155, 2011.

[8] F. Riss, J. Schilp and G. Reinhart, "Load-dependent Optimization of Honeycombs for Sandwich Components--New Possibilities by Using Additive Layer Manufacturing," *Physics Procedia,* vol. 56, pp. 327-335, 2014.

[9] D. Pollard, "Automated sandwich panel production utilising additive manufacture and silicone pick and place technology," Masters thesis, University of Bristol, 2014.

[10] J. White, J. Etches and C. Ward, "CDE 28088: The Development of Low Cost Additive Layer Manufacturing for Use as Repair Equipment in the Field, to Improve Operations and Support for Composite Platforms," 2013.

[11] D. Pollard, C. Ward, G. Herrmann and J. Etches, "The manufacture of honeycomb cores using Fused Deposition Modeling," *Advanced Manufacturing: Polmer & Composites Science*, vol 3, no. 1, pp. 21-31, 2017.

[12] Food and Drug Administration, Technical Considerations for Additive manufactured Devices, 2016.

[13] M. Yardimci, T. Hattori, S. Guceri and S. Danforth, "Thermal analysis of fused deposition," in *Proceedings of the Solid Freeform Fabrication Symposium, Austin*, 1997.

[14] A. Bellini, S. Guceri and M. Bertoldi, "Liquefier dynamics in fused deposition," *Journal of Manufacturing Science and Engineering,* vol. 126, no. 2, pp. 237-246, 2004.

[15] H. Ramanath, C. Chua, K. Leong and K. Shah, "Melt flow behaviour of poly-ε-caprolactone in fused deposition modelling," *Journal of Materials Science: Materials in Medicine,* vol. 19, no. 7, pp. 2541-2550, 2008.

[16] S. R. Stewart, J. E. Wentz and J. T. Allison, "Experimental and Computational Fluid Dynamic Analysis of Melt Flow Behavior in Fused Deposition Modelling of Poly (lactic) Acid," in *ASME 2015 International Mechanical Engineering Congress and Exposition*, 2015.

[17] C. Bellehumeur, L. Li, Q. Sun and P. Gu, "Modeling of bond formation between polymer filaments in the fused deposition modeling process," *Journal of Manufacturing Processes,* vol. 6, no. 2, pp. 170-178, 2004.

[18] Q. Sun, G. Rizvi, C. Bellehumeur and P. Gu, "Effect of processing conditions on the bonding quality of FDM polymer filaments," *Rapid Prototyping Journal,* vol. 14, no. 2, pp. 72-80, 2008.

[19] E3D, *E3D Hotend v6.*

[20] dSpace GmbH, *DS1103 PPC Controller Board,* 2008.

[21] FLIR, *FLIR ResearchIR Software.*